Available online at www.sciencedirect.com
SCIENCE DIRECT®
Journal of Computational Physics 191 (2003) 282–304
JOURNAL OF COMPUTATIONAL PHYSICS
www.elsevier.com/locate/jcp

Comparison of preconditioners for collocation Chebyshev approximation of 2D and 3D generalized Stokes problem

Abdou Garba [a,*], Pierre Haldenwang [b]

[a] Departamento de Matemática, Universidade Federal do Ceará Campus do Pici, Bl. 914, Cep: 60455-760 Fortaleza, CE, Brazil
[b] Laboratoire de Modélisation et Simulation Numérique en Mécanique, IMT/La Jetée/L3M, 38, Av. Fréderic Juliot–Curie, 13451 Marseille Cedex 20, France

Received 14 September 2002; received in revised form 7 April 2003; accepted 10 June 2003

Abstract

The aim of the paper is concerned with the iterative resolution of the generalized Stokes problem in the framework of collocation Chebyshev approximation. More precisely, we analyze the performance of several preconditioners improving the classical Uzawa method. We first recall that the general Stokes problem (GSP) is an elementary substep of general interest for computing not only incompressible flows but also low Mach number flows. We then remark that performances of the classical Uzawa algorithm for solving the GSP are in fact closely related to the Reynolds number. In order to overcome this dependence, preconditioners are needed. The preconditioners we analyze here are recommended by Fourier analysis of the pressure operator. We additionally give interpretation of the preconditioners in terms of influence (or capacitance) techniques. We give a detailed analysis of the conditioning of the discrete collocation Chebyshev versions of the operators. Numerical comparison is conducted in 2D as well as in 3D rectangular geometry. Our comparative study shows that the fictitious wall permeability (FWP) method is the most efficient preconditioner. If complemented with a suitable pressure filtering, its efficiency still increases.

Keywords: Generalized Stokes problem; Uzawa method; Preconditioned pressure operator; Chebyshev collocation method; Filtering for Chebychev spectral methods

1. Introduction

The computation of Navier–Stokes equations (NSEs) for incompressible flows (and also for low Mach number flow) is made difficult by the fact that pressure is not governed by an equation of evolution. In fact pressure serves as a field of Lagrange multiplier that ensures mass conservation. A wide diversity of ways

* Corresponding author. Tel.: +55-85-288-9890; fax: +55-85-288-9889.
E-mail addresses: garba@mat.ufc.br, abdgar@yahoo.fr (A. Garba), haldenwang@L3M.univ-mrs.fr (P. Haldenwang).

0021-9991/$ - see front matter © 2003 Elsevier B.V. All rights reserved.
doi:10.1016/S0021-9991(03)00317-6

for approximating NSEs exists in the literature. Almost invariably adopting a semi-implicit scheme for these equations leads to a sequence of generalized Stokes problems (GSPs). Therefore good solvers for the GSP are needed for efficient resolution of NSEs. Computational Fluid Dynamic literature on the subject is composed of two large classes of methods: projection methods and Uzawa algorithm based methods. Contrarily to projection methods, which are founded on the concept of an operator splitting applied to the unsteady Stokes problem (and involve some time stepping error), Uzawa's iterative method solves at each time step a steady problem as given in (12)–(14), and does not refer to any time stepping at that level. The present paper exclusively considers Uzawa's algorithm based methods. In the framework of spectral methods a classical way for solving the GSP is the influence matrix (or capacitance matrix) technique [1–3]. The influence matrix method is efficient for 2D problem. However because of excessive memory requirement and difficulties related to the inversion of the influence matrix, this method turns out to be inadequate for problem having a large amount of degrees of freedom at the boundary as in 3D-periodic situation. This is reason why, we shall first study an alternative which consists of an approximated influence relationship between pressure and incompressibility constraint on domain boundary, hereafter called approximated influence technique (AIT). Other alternatives have been proposed in the literature. Haldenwang [4,5] developed the fictitious wall permeability (FWP) method that also avoids the influence matrix; this method is hereafter denoted FWP. At the end of the 1980s, Cahouet and Chabard [6] have proposed a preconditioning that they qualified as "optimal" accordingly with an operator Fourier analysis. An implementation in the framework of finite elements confirmed the efficiency of the method hereafter denoted Cahouet and Chabard (CC) method. For sufficiently smooth solutions, it turns out that both AIT and CC methods have the same properties and the results for both methods will be refered to as CC/AIT method. The objective of the present work is mostly to carry out comparison between FWP method and CC/AIT method in the framework of pseudo-spectral Chebyshev discretization in 2D and 3D confined geometry.

The paper splits up into the following parts: in Section 2, we first show that the GSP is an elementary step for solving incompressible and also low Mach number (or dilatable) flows. We then derive in Section 3 the pressure operator and based on a heuristic operator analysis, we show that the Uzawa algorithm needs to be preconditioned for large Reynolds number. In Section 4, we present the preconditioned methods and interpret them as approximate influence techniques. In Section 5, we analyze the conditioning of the discrete 2D collocation Chebyshev version of the operators. The analysis is done by computing numerically the eigenvalues of the operators. Section 6 is devoted to numerical implementation of the algorithms. We compare the convergence of the various algorithms in both 2D and 3D situations. Finally we implement a filtering procedure that allow an enhancement of the FWP algorithm.

2. Generalized Stokes problem

In this section we show how the GSP arises as part of solution process of incompressible and compressible NSEs in bounded domain when semi-implicit treatment is adopted for time-advancing.

2.1. Incompressible flow

Let Ω be a bounded domain in $\mathbb{R}^d$ $(d = 2, 3)$. We consider the incompressible NSEs in Ω:

$$\partial_t \mathbf{u} - \nu \Delta \mathbf{u} + \nabla p = -(\mathbf{u} \cdot \nabla)\mathbf{u} + \mathbf{f}, \tag{1}$$

$$\nabla \cdot \mathbf{u} = 0, \tag{2}$$

where $\mathbf{u}$ is the velocity field, p is the pressure, ν is the viscosity and $\mathbf{f}$ is an external force. We consider also initial condition and for the shake of simplicity Dirichlet boundary conditions for the velocity field. Usually

a semi-implicit discretization is used for the diffusive part of (1) and the advective part is discretized in an explicit manner. Then, the following GSP is to be solved at each time step

$$\alpha\mathbf{u} - v\Delta\mathbf{u} + \nabla p = \mathbf{F}, \tag{3}$$

$$\nabla \cdot \mathbf{u} = 0, \tag{4}$$

where the coefficient α is proportional to the inverse of Δt the time step, $\mathbf{F}$ is a known vector field that depends on extrapolations of velocities from previous times. The time stepping is typically limited by CFL-like conditions based on the first derivatives contained in the explicit part (i.e., in the advection terms).

2.2. Flow at low Mach number

An equivalent system that concerns a momentum–pressure formulation can be derived for dilatable flows when using a semi-implicit treatment that exhibits the same CFL limitation on time stepping. Starting now from the compressible NSEs:

$$\partial_t(\varrho\mathbf{u}) - \mu\Delta\mathbf{u} + \nabla p = \frac{\mu}{3}\nabla(\nabla \cdot \mathbf{u}) - \nabla \cdot (\varrho\mathbf{u} \otimes \mathbf{u}) + \mathbf{f}, \tag{5}$$

$$\nabla \cdot (\varrho\mathbf{u}) = -\partial_t\varrho, \tag{6}$$

where ϱ is the density, μ the viscosity coefficient and as before, initial and boundary conditions are prescribed for the velocity field. Because density variations with respect to pressure fluctuations in the flow are proportional to the square of the Mach number, one assumes in the low Mach number approximation that fluid density only depends on average pressure, this is, thermodynamic pressure (and also on scalar variables as temperature). In other words, dynamic pressure has a negligible influence on density variations. Therefore the right-hand side of (6) is determined by integrating scalar equations [7]. For instance, when a semi-implicit discretization is used, one can consider that the density field is known at time level $n+1$ by integrating the equation of energy. Thus, temporal and spatial derivatives of density are known at time level $n+1$ thanks to a semi-implicit scheme with the same CFL-like stability criterion. We consider now the vector identity:

$$\Delta\mathbf{u} = \frac{1}{\varrho}\Delta(\varrho\mathbf{u}) - \frac{1}{\varrho}(\Delta\varrho)\mathbf{u} - \frac{2}{\varrho}\nabla\varrho \cdot \nabla\mathbf{u}. \tag{7}$$

We claim that in fact, a not more unstable time scheme on the viscous part is obtained when (7) is discretized as

$$\Delta\mathbf{u} = \frac{1}{\varrho}\Delta(\varrho\mathbf{u}) - \mathbf{f}_1^{n,\cdots}, \tag{8}$$

where $\mathbf{f}_1^{n,\cdots}$ only contains extrapolations at time $n+1$ of the velocity and its first derivatives from the previous times. This transformation allows us to introduce at time level $n+1$ an implicit term of dissipation related to momentum diffusion, the coefficient of which is kinematic viscosity. Furthermore, the velocity divergence at time level $n+1$ can be estimated from the continuity (6) as

$$\nabla \cdot \mathbf{u} = h \equiv \left\{ \frac{1}{\varrho}(\nabla\varrho \cdot \mathbf{u} - \partial_t\varrho) \right\}^{n+1,n,\cdots}. \tag{9}$$

Remark that the right-hand side of (9) can be estimated with extrapolations of velocity field that are stable since no velocity derivatives are involved. Taking the gradient of (9), one obtains an explicit estimate of the

viscous dissipative term related to volumic expansion. It is worth noticing that the latter extrapolation only contains the first derivatives of velocities. Therefore this explicit treatment of the volumic viscous term is concerned with the same type of CFL-like stability criterion. Actually, if the pressure field is not needed, the volumic viscous term can be incorporated with pressure (we can then set $h = 0$). Taking into account all the above semi-implicit treatments, we get at time $n+1$ the following "unsteady" Stokes problem for the momentum–pressure formulation:

$$\partial_t(\varrho\mathbf{u}) - \frac{\mu}{\varrho}\Delta(\varrho\mathbf{u}) + \nabla p = \mathbf{F} \equiv \left\{ -\mu\mathbf{f}_1 + \frac{\mu}{3}\nabla(h) - \nabla\cdot(\varrho\mathbf{u}\otimes\mathbf{u}) + \mathbf{f} \right\}^{n+1,n,\ldots}, \tag{10}$$

$$\nabla\cdot(\varrho\mathbf{u}) = g \equiv \{-\partial_t\varrho\}^{n+1}, \tag{11}$$

where $\mathbf{F}$ is a vector field that, at most, contains extrapolations of velocity first derivatives from previous times. Consequently, time integration of (10) leads to a GSP problem that is formally identical to the one defined by (3) and (4). The only difference could be in the variation of the viscosity coefficient $v = \mu/\varrho$. This difficulty can however be avoided by just retaining a constant viscosity v_0 in the left-hand side of (10) and by transferring the fluctuating viscosity $v - v_0$ in the right-hand side of the equation. The latter quantity then appears as the viscosity coefficient of an extrapolation at time $(n+1)\Delta t$ of the momentum Laplacian. The procedure leading to the Stokes problem defined by (10) and (11) has already received two successful applications: Non-Boussinesq convective flows by Fröhlich and Peyret [8] and flows with combustion by Denet and Haldenwang [9].

3. Pressure operator and Uzawa algorithm

Instead of solving a large system that arises from the time discretization of GSP, it has been recognized for a long time that iterative procedures that solve a cascade of elliptic problems is an efficient way to split up the former system. The construction of such iterative procedures is based on the analysis of the pressure operator. In this section we present the pressure operator and, anticipating numerical results, we give an heuristic analysis of the conditioning of the operator. Let us consider the GSP problem in Ω a bounded domain in $\mathbb{R}^d$ $(d = 2, 3)$ with boundary Γ:

$$\alpha\mathbf{u} - v\Delta\mathbf{u} + \nabla p = \mathbf{F}, \tag{12}$$

$$\nabla\cdot\mathbf{u} = 0, \tag{13}$$

with Dirichlet boundary conditions

$$\mathbf{u} = \mathbf{u}_\Gamma \quad \text{on } \Gamma. \tag{14}$$

In the continuity constraint (13) we have considered a homogeneous right-hand side only for simplicity of the the presentation. Let $\mathscr{I}$ be the identity operator. We define formally $\mathscr{H}_{\mathrm{D}}$ to be the Helmholtz operator

$$\mathscr{H}_{\mathrm{D}} \equiv (\alpha\mathscr{I} - v\Delta)_{\mathrm{D}}, \tag{15}$$

equipped with Dirichlet boundary conditions. It is well known that $\mathscr{H}_{\mathrm{D}}$ is invertible and therefore we can solve (12) subject to boundary condition (14) for $\mathbf{u}$:

$$\mathbf{u} = \mathscr{H}_D^{-1}(\tilde{\mathbf{F}} - \nabla p), \tag{16}$$

where $\tilde{\mathbf{F}}$ is a modified right-hand side that takes accounts non-homogeneous boundary conditions. Inserting expression (16) of $\mathbf{u}$ in the continuity (13), we get

$$\nabla \cdot \mathbf{u} = \nabla \cdot \mathscr{H}_D^{-1}(\tilde{\mathbf{F}} - \nabla p) = 0. \tag{17}$$

This leads to a linear equation for pressure

$$\mathscr{A} p = g \equiv -\nabla \cdot \mathscr{H}_D^{-1}(\tilde{\mathbf{F}}), \tag{18}$$

where pressure operator $\mathscr{A}$ is defined by

$$\mathscr{A} \equiv -\nabla \cdot \mathscr{H}_D^{-1} \nabla. \tag{19}$$

If the weak formulation of problem (12)–(14) is considered, it can be shown that operator $\mathscr{A}$ is symmetric, positive definite from $L_0^2(\Omega)$ to $L_0^2(\Omega)$ (cf. [10] for instance), where $L_0^2(\Omega)$ is the space of square integrable functions in Ω with zero mean

$$L_0^2(\Omega) \equiv \left\{ \phi \in L^2(\Omega) \Big/ \int_\Omega \phi = 0 \right\}.$$

Thus, iterative methods of gradient type can be apply to solve problem (12)–(14). The simplest iterative method for solving the GSP is the classical Uzawa algorithm which can be sumarized as follows:

1. Chose an initial guess p^0.
2. For $m \geqslant 0$ repeat steps 2.1 and 2.2 until convergence is reached:
   2.1. solve $\mathscr{H}_{\mathrm{D}}(\mathbf{u}^m) = \mathbf{F} - \nabla p^m$,
   2.2. relaxation: $p^{m+1} = p^m + \varrho_{m+1}(g - \mathscr{A} p^m) = p^m - \varrho_{m+1} \nabla \cdot \mathbf{u}^m$.

The integer m above is the iterations counter and ϱ_{m+1} is a relaxation parameter. The convergence of Uzawa algorithm is guaranteed provided the relaxation parameter is sufficiently small. The performance of the algorithm is fairly good for small values of the ratio $\sigma = \alpha/\nu$. However for large values of σ, the convergence of the algorithm is very slow due to the bad-conditioning of the pressure operator. This is unfortunately the case in most situations of interest where the Reynolds number is high (say ν small) and the time step Δt must be taken small for CFL stability reasons. A qualitative analysis of the conditioning of the discrete collocation Chebyshev version of $\mathscr{A}$ is presented in Section 5 in 2D case. However we can for the time being give an heuristic analysis that is helpful to understand the behavior of the Uzawa algorithm.

Indeed if $\sigma = \alpha/\nu$ is small (i.e., $\sigma \ll 1$), neglecting the boundary conditions, we can make the following estimate for operator $\mathscr{A}$:

$$\mathscr{A} = -\nabla \cdot (\alpha \mathscr{I} - \nu \Delta)^{-1} \nabla = -\frac{1}{\nu} \nabla \cdot (\sigma \mathscr{I} - \Delta)^{-1} \nabla \simeq \frac{1}{\nu} \nabla \cdot \Delta^{-1} \nabla. \tag{20}$$

If we make the heuristic assumption that the operators in the right-hand side of (20) commute with each other (this is true for periodic boundary conditions) we obtain

$$\mathscr{A} \simeq \frac{1}{\nu} \mathscr{I}, \tag{21}$$

i.e., $\mathscr{A}$ behaves like a constant times unity operator, therefore one expects a fairly good convergence of the Uzawa algorithm if σ is small. On the other hand if $\sigma \gg 1$ we have

$$\mathscr{A} = -\frac{1}{\alpha} \nabla \cdot \left(\mathscr{I} - \frac{1}{\sigma} \Delta \right)^{-1} \nabla \simeq -\frac{1}{\alpha} \Delta. \tag{22}$$

This time, $\mathscr{A}$ behaves like the Laplacian operator. It is well known that the eigenvalues of the second order derivation operator grow like $\mathscr{O}(N^2)$ for finite elements method or Fourier method and $\mathscr{O}(N^4)$ for Chebyshev method, where N is the degree of freedom. Thus one expects a slow convergence of the Uzawa

algorithm if σ is large. In conclusion, preconditioner is needed in order to obtain effective iterative solvers if σ is large. In what follows, we present several preconditioning methods for the Uzawa algorithm.

4. The preconditioned methods

If we assume heuristically that divergence operator nearly commutes with the inverse of Helmholtz operator we can approximate operator $\mathscr{A}$ as

$$\mathscr{A} = -\nabla \cdot \mathscr{H}_{\mathrm{D}}^{-1} \nabla \simeq -\mathscr{H}_{\mathrm{D}}^{-1} \Delta. \tag{23}$$

The commutativity holds if periodic boundary conditions were considered. Indeed, let us assume that the problem is periodic with period length L in all directions. We then introduce the Fourier expansions of $\mathbf{u}$ and p:

$$\mathbf{u}(\mathbf{x}) = \sum_{\mathbf{k} \in Z^d} \mathbf{u}_{\mathbf{k}} \mathrm{e}^{2\underline{\mathrm{i}}\pi \mathbf{k} \cdot \mathbf{x}/L}, \quad p(\mathbf{x}) = \sum_{\mathbf{k} \in Z^d} p_{\mathbf{k}} \mathrm{e}^{2\underline{\mathrm{i}}\pi \mathbf{k} \cdot \mathbf{x}/L}, \qquad d = 2, 3, \tag{24}$$

where $\underline{\mathrm{i}}^2 = -1$. The momentum (12) (setting $\mathbf{F} = \mathbf{0}$) reduces to

$$\left(\alpha + \frac{4\pi^2 |\mathbf{k}|^2 \nu}{L^2} \right) \mathbf{u}_{\mathbf{k}} = -\frac{\underline{\mathrm{i}} 2\pi \mathbf{k}}{L} p_{\mathbf{k}}, \quad \mathbf{k} \in Z^d, \tag{25}$$

and the divergence operator reduces to

$$(\nabla \cdot \mathbf{u})_{\mathbf{k}} = \frac{\underline{\mathrm{i}} 2\pi}{L} \mathbf{k} \cdot \mathbf{u}_{\mathbf{k}}, \ \mathbf{k} \in Z^d. \tag{26}$$

Taking the scalar product of (25) with $\underline{\mathrm{i}} 2\pi \mathbf{k}/L$ and using (26), we see that in the Fourier space the relation $\mathscr{A} p = -\nabla \cdot \mathbf{u}$ takes the simple form

$$\mathscr{A}_{\mathbf{k}} p_{\mathbf{k}} = \lambda_{\mathbf{k}} p_{\mathbf{k}}, \tag{27}$$

where

$$\lambda_{\mathbf{k}} = \frac{4\pi^2 |\mathbf{k}|^2}{4\pi^2 |\mathbf{k}|^2 \nu + \alpha L^2}. \tag{28}$$

In the same way, one can easily show that operator

$$\mathscr{C}_1 \equiv -(\alpha \mathscr{I} - \nu \Delta)^{-1} \Delta = -\mathscr{H}^{-1} \Delta \tag{29}$$

associated with the same periodic boundary conditions reduces to (27) with the $\lambda_{\mathbf{k}}$'s given by (28). Thus, in case of periodicity conditions, the equality $\mathscr{A} = \mathscr{C}_1$ is true. However, in the general case the different operators in the expression of $\mathscr{A}$ do not commute because of the boundary conditions. This is particularly true for the discrete version of the operators. Nevertheless one expects the operator $\mathscr{C}_1$ to provide a reasonable approximation for $\mathscr{A}$ at the interior points. Let us consider operator $\mathscr{C}_1$ defined by (29) as preconditioner for $\mathscr{A}$. The preconditioning process consists then in replacing step 2 in the Uzawa algorithm (see Section 3) by

$$\mathscr{H}_{\mathrm{D}}^{-1} \Delta (p^{m+1} - p^m) = \varrho_{m+1} (g - \mathscr{A} p^m) = -\varrho_{m+1} \nabla \cdot \mathbf{u}^m. \tag{30}$$

Applying operator $\mathscr{H}$ to both sides of (30) leads to the Poisson equation

$$\Delta(\delta p^{m+1}) = -\mathscr{H}(\nabla \cdot \mathbf{u}^m) \quad \text{in } \Omega, \tag{31}$$

for the pressure correction (or increment)

$$\delta p^{m+1} \equiv \frac{p^{m+1} - p^m}{\varrho_{m+1}}. \tag{32}$$

Boundary conditions for (31) will be presented later. It follows from (31) that if the iterative process converges (i.e., $\delta p^m \to 0$), one forces the divergence of the velocity to be solution of an homogeneous Helmholtz equation. Therefore the divergence will be identically zero if it satisfies some homogeneous boundary conditions (for example Dirichlet or Neumann conditions). We then extend the initial GSP in the Following manner: the continuity constraint must be satisfied up to the domain boundary (which is true for classical solution).

Many authors used the influence matrix technic in which pressure distribution on the boundary is determined so as to satisfy the continuity constraint on the boundary Γ. A detailed analysis and implementation of this method can be found in [1–3] in the framework of spectral approximations. In situations where this technique can be applied, it leads to very accurate solution. However the influence matrix method is efficient only in case of Stokes problems with constant coefficients and when the problem has to be solved many times. Furthermore, the dimension of the influence matrix grows like the number of the boundary points, this is $2(N_1 + N_2)$ for 2D problems and $2(N_1N_2 + N_1N_3 + N_2N_3)$ for 3D problems, where N_i, $i = 1, 2, 3$ are the degrees of discretization in the respective directions. Due to its excessive memory requirement as well as inaccuracy related to the inversion of the matrix of influence, this technic is prohibitive in 3D situations. In the next three sections, we present several approaches that avoid recourse to influence matrix.

4.1. The approximated influence technique (AIT)

In Computational Fluid Dynamic literature, Poisson equation is often used to compute (or correct) pressure field and the problem of closing this PDE with suitable boundary conditions is invariably addressed. Most of the time boundary conditions for pressure are deduced from the normal component of the momentum equation on the boundary. Here we need to complement (31) with boundary conditions that ensure at convergence a divergence free velocity field. To start with, let us notice that from (12) it follows that

$$\frac{\partial p}{\partial n} = (\mathbf{F} - \alpha\mathbf{u}) \cdot \mathbf{n} + \nu \left[\frac{\partial(\nabla \cdot \mathbf{u})}{\partial n} - \nabla \times (\nabla \times \mathbf{u}) \cdot \mathbf{n} \right] \quad \text{on } \Gamma, \tag{33}$$

where $\mathbf{n}$ is the unit normal vector on Γ. In the present method, we propose to drop the term $\nabla \times (\nabla \times \mathbf{u}) \cdot \mathbf{n}$ in the right-hand side of (33) and consider the following approximated equation:

$$\frac{\partial p}{\partial n} \simeq (\mathbf{F} - \alpha\mathbf{u}) \cdot \mathbf{n} + \nu \frac{\partial(\nabla \cdot \mathbf{u})}{\partial n} \quad \text{on } \Gamma. \tag{34}$$

Now we write (34) at iterations $m + 1$ and m and subtract the two resulting expressions. Furthermore if we assume (heuristically) that $\nabla \cdot \mathbf{u}^{m+1}$ is small with respect to $\nabla \cdot \mathbf{u}^m$, we get the following boundary conditions:

$$\frac{\partial(\delta p^{m+1})}{\partial n} = -\nu \frac{\partial(\nabla \cdot \mathbf{u}^m)}{\partial n} \tag{35}$$

for (31). The fact of the matter is that, if the overall process converges (i.e., $\delta p^{m+1} \to 0$), the divergence field is solution of a homogeneous Helmholtz equation (right-hand side of (31)) with homogeneous Neumann boundary condition (right-hand side of (35)).

In contrast to influence matrix technique where boundary conditions for the pressure are determined so that $\nabla \cdot \mathbf{u} = 0$ on Γ (35), involves proportionality between two local quantities at the wall. It indeed corresponds to a poorer influence relationship between pressure and divergence at the wall. This is why we suggest the name "approximated influence technic (AIT)" for this first preconditioning.

Remark. If $\sigma = \alpha/\nu \simeq 0$, it follows from (31) and (35) that $\delta p^{n+1} \simeq -\nu \nabla \cdot \mathbf{u}^{n+1}$, which means that the AIT preconditioner behaves like a constant times unity operator. Therefore the AIT preconditioning has little effect if σ is small.

4.2. The fictitious wall permeability method

The FWP method was developed [4,5] in the same context as the AIT method, i.e., how to impose the continuity constraint on the boundary of the domain? To this end we note that if the continuity constraint is assumed to be satisfied up to the boundary of the domain (which is true for classical solution), supplementary boundary condition is obtained for the velocity field. Thus in situations where the normal velocity is always one of the velocity components (for example in rectangular geometries), one may solve the momentum (12) for the velocity field with the following boundary conditions:

- Original Dirichlet conditions (14) when the velocity component is parallel to the wall.
- Neumann conditions when the velocity component is normal to the wall.

Thus the Neumann condition on the normal velocity,

$$\frac{\partial u_n}{\partial n} = -\nabla_t \cdot \mathbf{u}_t, \tag{36}$$

is related to the tangential part of the velocity divergence (known at the wall: $\nabla_t \cdot \mathbf{u}_t = \nabla_t \cdot (\mathbf{u}_\Gamma)_t$) and permits to enforce the continuity constraint on the boundary of the domain. Hereafter subscripts t and n refer, respectively, to tangential and normal quantities.

To be concrete, let us consider the case where Ω is the square domain $(-1,1) \times (-1,1)$ in $\mathbb{R}^2$ and the velocity components are u, v in the x and y directions respectively. Then at each iteration one solves for u the momentum (12) associated with Dirichlet conditions

$$u^m = u_\Gamma \tag{37}$$

on the sides $x = -1$ and $x = 1$ and Neumann conditions

$$\frac{\partial u^m}{\partial x} = -\frac{\partial v_\Gamma}{\partial y} \tag{38}$$

on the sides $y = -1$ and $y = 1$. For the y component of the velocity one solves the momentum (12) subjected to Dirichlet conditions

$$v^m = v_\Gamma \tag{39}$$

on the sides $y = -1$ and $y = 1$ and Neumann conditions

$$\frac{\partial v^m}{\partial y} = -\frac{\partial u_\Gamma}{\partial x} \tag{40}$$

on the other sides. The iterative process includes step (31) for the computation of the pressure increment δp^{m+1}. Therefore, after convergence of the algorithm the divergence field satisfies an homogeneous Helmholtz equation. This ensures the divergence free condition in the whole domain since by construction the divergence is zero on the boundary. The remaining point is to impose the original Dirichlet condition

(14) on the velocity components normal to the boundary. This is achieved by duality thanks to boundary condition on the pressure correction

$$\frac{\partial(\delta p^{m+1})}{\partial n} = \mathscr{H}_t(u_n^m - (u_\Gamma)_n), \tag{41}$$

which are derived from an approximation of the normal projection of the momentum equation on the boundary. In (41), $\mathscr{H}_t \equiv \alpha\mathscr{I} - \nu\Delta_t$ and Δ_t is the tangential part of the Laplacian operator. It follows from (41) that after convergence of the iterative process one has solved for $u_n - (u_\Gamma)_n$ the homogeneous Helmholz problem

$$\mathscr{H}_t(u_n - (u_\Gamma)_n) = 0 \tag{42}$$

with homogeneous Dirichlet boundary conditions on each side of the domain. This ensures that $u_n = (u_\Gamma)_n$ on the boundary. Thus, after convergence, all equations of the GSP (12)–(14) are satisfied.

No theoretical convergence property of FWP algorithm has yet been proved. However, numerical experiments in the case of spectral Chebyshev Tau method [4,5] show a fast rate of convergence of the algorithm.

Remark. If the boundary conditions are impermeable(this is $(u_\Gamma)_n = 0$) then the FWP method allows the boundary to be initially permeable (i.e., u_n^m is not necessary zero on Γ in the first iterations). The impermeability condition is obtained only after convergence of the algorithm. The name "fictitious wall permeability" of the method originates from this fact.

4.3. The Cahouet and Chabard method

In the periodic case the eigenvalues of operator $\mathscr{A}$ are $\lambda_{\mathbf{k}} = 4\pi^2|\mathbf{k}|^2/(4\pi^2|\mathbf{k}|^2\nu + \alpha L^2)$ (see (27) and (28)). When they are rewritten into the form $\lambda_{\mathbf{k}} = (\nu + \alpha/4\pi^2|\mathbf{k}|^2)^{-1}$, these eigenvalues may also be seen as those of the operator

$$\mathscr{C}_2 \equiv (\nu\mathscr{I} - \alpha\Delta^{-1})^{-1}. \tag{43}$$

This observation led Cahouet and Chabard [6] to consider operator (43) as preconditioner for $\mathscr{A}$. Then the CC procedure consists in substituting Step 3 in the Uzawa algorithm (cf. Section 2.3) by

$$p^{m+1} = p^m - \varrho_{m+1}(\nu\mathscr{I} - \alpha\Delta_{\mathrm{b}}^{-1})(\nabla\cdot\mathbf{u}^m), \tag{44}$$

where Δ_{b}^{-1} is the inverse of the Laplacian operator with Neumann boundary conditions. More precisely at iteration $m+1$ the authors [6] solve the Poisson equation

$$\Delta\varphi^{m+1} = \nabla\cdot\mathbf{u}^m \quad \text{in } \Omega \tag{45}$$

with homogeneous Neumann boundary conditions

$$\frac{\partial\varphi^{m+1}}{\partial n} = 0 \quad \text{on } \Gamma, \tag{46}$$

then set

$$\delta p^{m+1} = \alpha\varphi^{m+1} - \nu\nabla\cdot\mathbf{u}^m. \tag{47}$$

When finite elements method is associated with the conjugated gradient method, Cahouet and Chabard [6] found that the rate of convergence of the algorithm does not depend on the degree of approximation.

Actually the CC method may be interpreted in term of approximated influence technique. More precisely, we have:

Proposition 1. *For sufficiently smooth solution, the CC method and the AIT method are equivalent.*

Proof. We assume that the divergence is sufficiently smooth and we take the Laplacian of both sides of (47)

$$\Delta(\delta p^{m+1}) = \alpha\Delta\varphi^{m+1} - \nu\Delta(\nabla\cdot\mathbf{u}^m). \tag{48}$$

Using (45) in (48) we see that δp^{m+1} satisfies the Poisson (31). Furthermore by taking the normal derivative of (47) and using (46) one gets the boundary conditions (35) for δp^{m+1}. On the other hand, if δp^{m+1} satisfies (31) then $\varphi^{m+1} = (\delta p^{m+1} + \nu\nabla\cdot\mathbf{u}^m)/\alpha$ is solution of the Poisson problem (45) and (46). Thus the two formulations (31), (35) and (45), (47) are equivalent.

4.4. Description of the iterative procedures

Here we give the description of the iterative algorithms. In order to allow for dynamical choices of the relaxation parameter, we introduce also a correction term $\delta\mathbf{u}^{m+1}$ for the velocity. The preconditioned algorithms can be summarized as follows:

1. Initialization:
   1.1. Choose p^0.
   1.2. Solve $\mathscr{H}_\mathrm{b}(\mathbf{u}^0) = \tilde{\mathbf{F}} - \nabla p^0$.
2. Iterations: $(\mathbf{u}^m, p^m)$ are known:
   2.1. Solve $\Delta_\mathrm{b}(\delta p^{m+1}) = \mathscr{H}(\nabla\cdot\mathbf{u}^m)$.
   2.2. Solve $\mathscr{H}_\mathrm{b}(\delta\mathbf{u}^{m+1}) = -\nabla(\delta p^{m+1})$.
   2.3. Compute ϱ_{m+1}.
   2.4. Relaxation: $p^{m+1} = p^m + \varrho_{m+1}\delta p^{m+1}$, $\mathbf{u}^{m+1} = \mathbf{u}^m + \varrho_{m+1}\delta\mathbf{u}^{m+1}$.
   2.5. If $\|\nabla\cdot\mathbf{u}^{m+1}\| \leqslant \varepsilon$, then $\mathbf{u} = \mathbf{u}^{m+1}$ else return to step 2.1.

The parameter ε is a criterion of convergence. Here $\mathscr{H}_\mathrm{b}$ stands for the Helmholtz operator supplemented with the appropriate boundary conditions (i.e., Dirichlet conditions for the CC/AIT method, Dirichlet/Neumann conditions in 2D and Dirichlet/Dirichlet/Neumann conditions in 3D for the FWP method) and Δ_b is the Laplace operator with appropriate Neumann boundary conditions. The parameter ϱ_{m+1} is the relaxation parameter. Because of the non-symmetrical formulation of the Chebyshev collocation methods, our iterative procedures cannot use conjugated gradient method. We have implemented three different methods for selecting the relaxation parameter. The simplest choice is the Richardson method in which ϱ_{m+1} is kept constant during the iterations. The best choices of the parameter ϱ are determined by numerical tests. We also have considered two dynamical methods for choosing the relaxation parameter. The first method is the preconditioned minimal residual (PMR) technique where at each iteration ϱ_m is computed in order to minimize the residual. This leads to

$$\varrho_{m+1} = \frac{\langle\nabla\cdot\mathbf{u}^m, \nabla\cdot\delta\mathbf{u}^{m+1}\rangle}{\langle\nabla\cdot\delta\mathbf{u}^{m+1}, \nabla\cdot\delta\mathbf{u}^{m+1}\rangle}, \tag{49}$$

where $\langle\cdot\rangle$ stands for the Euclidian inner product. In some cases (namely when σ is small) we have observed that when the PMR method is used, the FWP algorithm stagnates too soon. To remedy such a situation, we have implemented an alternative method in which the relaxation parameter is taken as

$$\varrho_{m+1} = \frac{\|\nabla \cdot \mathbf{u}^m\|}{\|\nabla \cdot \delta\mathbf{u}^{m+1}\|}, \tag{50}$$

where $\|\cdot\|$ is the Euclidian norm. Unlike the PMR method, the latter choice of the relaxation parameter is not optimal. However, when the method is associated to a good preconditioning, it leads to a significant decrease of the residual at each iteration. This method will be refered to as the quasi-preconditioned minimal residual (QPMR) method for reasons that will be justified next.

4.4.1. Analysis of the quasi-minimal residual method

Let us consider the general linear problem

$$\mathscr{A}\varphi = f. \tag{51}$$

One iteration of a preconditioned iterative method for solving (51) consists of the following steps:

1. solve $\mathscr{A}_0\delta\varphi^{m+1} = \mathscr{R}^m \equiv f - \mathscr{A}\varphi^m$,
2. then set $\varphi^{m+1} = \varphi^m + \varrho\delta\varphi^{m+1}$,
3. and $\mathscr{R}^{m+1} = \mathscr{R}^m - \varrho\mathscr{A}\delta\varphi^{m+1}$,

where $\mathscr{A}_0$ is a preconditioner for $\mathscr{A}$, ϱ is the relaxation parameter and $\mathscr{R}^m$ is the residual at iteration m. From step 3, the square of the Euclidian norm of the residual $\mathscr{R}^{m+1}$ is given by

$$\|\mathscr{R}^{m+1}\|^2 = \|\mathscr{R}^m\|^2 - 2\varrho\langle\mathscr{R}^m, \mathscr{A}\delta\varphi^{m+1}\rangle + \varrho^2\|\mathscr{A}\delta\varphi^{m+1}\|^2. \tag{52}$$

In the case of the PMR method the parameter ϱ is chosen in order to minimize the quantity $\|\mathscr{R}^{m+1}\|$. This leads to (49) in the specific case of the GSP. In the case of the general linear system (51), the choice (50) for the QPMR method corresponds to

$$\varrho = \frac{\|\mathscr{R}^m\|}{\|\mathscr{A}\delta\varphi^{m+1}\|} = \frac{\|\mathscr{A}_0\delta\varphi^{m+1}\|}{\|\mathscr{A}\delta\varphi^{m+1}\|}. \tag{53}$$

If we substitute (53) in (52) we get

$$\|\mathscr{R}^{m+1}\|^2 = 2\|\mathscr{R}^m\|^2(1 - \langle\vec{u},\vec{v}\rangle), \tag{54}$$

where $\vec{u}$ and $\vec{v}$ are the unitary vectors in the directions of $\mathscr{A}\delta\varphi^{m+1}$ and $\mathscr{A}_0\delta\varphi^{m+1}$, respectively. If the preconditioner $\mathscr{A}_0$ is a good approximation of $\mathscr{A}$, one has $\langle\vec{u},\vec{v}\rangle \simeq 1$ so that the reduction factor $\beta_{\mathrm{QPMR}} = \sqrt{2(1 - \langle\vec{u},\vec{v}\rangle)}$ of the residual is close to zero. In practice one reasonably expects a reduction factor at least smaller than one at each iteration, guaranteeing the convergence of the method. Observe that in the case of the PMR method, the same calculation lead to a reduction factor $\beta_{\mathrm{PMR}} = \sqrt{1 - \langle\vec{u},\vec{v}\rangle^2}$. If we assume that $\langle\vec{u},\vec{v}\rangle \simeq 1$, we get $\beta_{\mathrm{PMR}} \simeq \sqrt{2(1 - \langle\vec{u},\vec{v}\rangle)}$. Thus with a good preconditioner the rate of convergence of the QPMR method is similar to that of PMR method .

Let us mention that the QPMR method have been used in [11] for the computation of free surface flow and in situations where the solution is stiff this method is found to be more robust than the PMR method.

Before we go through the numerical implementation of the algorithms, we give a qualitative analysis of the conditioning of the various operators.

5. Eigenvalues analysis

In this section we analyze the conditioning of the discrete collocation Chebyshev versions of the operators. This is done in the 2D case. The discretization is based on the Gauss–Lobatto points

$$\eta_j = \cos(j\pi/N), \quad j = 0, \ldots, N, \tag{55}$$

where for simplicity equal discretization is considered in both directions (this is $N_x = N_y = N$). The entire spectrum can be found after explicit construction of the discrete operators. The operators can be constructed numerically by solving a sequence of $(N+1)^2$ elementary problems corresponding to one step of the algorithms. For example to obtain the $\{(N+1)*(j-1)+i\}$th column L_{ij} $(0 \leqslant i, j \leqslant N)$ of the non-preconditioned pressure operator, we first compute

$$\mathbf{u}_{ij} = \mathscr{H}_{\mathrm{b}}^{-1}(-\nabla p_{ij}),$$

where p_{ij} is a pressure field with values 1 at the collocation point $[\cos(i\pi/N), \cos(j\pi/N)]$ and 0 elsewhere. Then the column L_{ij} is obtained by taking the divergence of $\mathbf{u}_{ij}$:

$$L_{ij} = \nabla \cdot \mathbf{u}_{ij}.$$

For the preconditioned operators, the corresponding column L_{ij} is obtained by solving in addition the Poisson equation

$$\Delta_{\mathrm{b}}(L_{ij}) = \mathscr{H}(\nabla \cdot \mathbf{u}_{ij})$$

with the appropriated boundary conditions.

The eigenvalues may also be found by the following procedure. If we unfold (rowwise for instance) the discrete 2D pressure field as 1D vector of length $(N+1)^2$, then the collocation derivative operators can be represented as square matrices of order $(N+1)^2 \times (N+1)^2$. In this way the construction of the discrete versions of the operators $\mathscr{H}$, $\mathscr{A}$ and Δ_{b} is straightforward. Then the eigenvalues of the non-preconditioned operator may be computed in a direct way and those of the preconditioned operators may be obtained by solving the generalized eigenvalues problem $\mathscr{H}\mathscr{A}(\varphi) = \lambda\Delta_{\mathrm{b}}(\varphi)$.

We have used both methods to compute the eigenvalues. The results we obtained are identical up to machine precision.

The spectrum of the non-preconditioned pressure operator as well as those of the Preconditioned operators contain 8 zero eigenvalues. These zero eigenvalues are related to the well-known spurious modes that are associated to the Gauss–Lobatto discretization of the Stokes problem (cf. [14, p. 235] for instance). Note however that in the present situation, the spurious modes have no influence on the convergence of the iterative process since the same modes in the right-hand side $\nabla \cdot \mathscr{H}^{-1}(\tilde{\mathbf{F}})$ of (18) are filtered by the divergence operator.

In Fig. 1, we plotted the eigenvalues of the three operators for the cases $\sigma = 1$ and $\sigma = 1000$ and with the discretization $N = 20$. A few of them are complex with small(relatively to the real parts) imaginary parts. The real parts of the eigenvalues of the operators are non-negative and belong to interval $[0, 1]$. (They belong to $[0, 1[$ in the case of the non-preconditioned operator.) The distribution of the real parts of the eigenvalues can be seen in Fig. 2. For small value of σ ($\sigma = 1$) most of the eigenvalues of the non-preconditioned pressure operator as well as those of the preconditioned operator are clustered about unity. This confirms the fairly good convergence of the Uzawa algorithm for small σ. In this case the preconditionings do not significantly alter the spectrum of the non-preconditioned operator.

If we switch to the large value $\sigma = 1000$, the distribution of the eigenvalues of non-preconditioned pressure operator changes drastically. Now the eigenvalues of the operator are somehow uniformly distributed in the interval $[0, 7[$ and only a few of them are clustered about value 0.9. This clearly indicates the ill-conditioning of the non-preconditioned pressure operator for large σ. However, applying the preconditionings results again to a clustering of the eigenvalues about unity.

Actually in both the cases $\sigma = 1$ and $\sigma = 1000$, more than three quarters of spectrum of the preconditioned operators is constituted of eigenvalues unity. Nevertheless a relatively small number of the

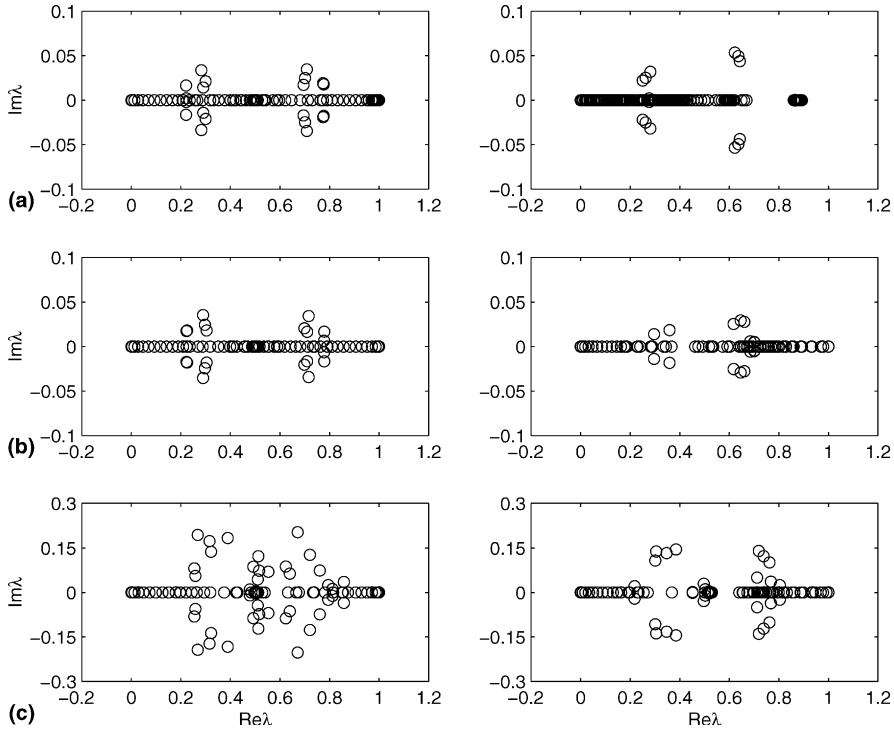

Fig. 1. Eigenvalues distribution of the pressure operator (a), the CC/AIT operator (b) and the FWP operator (c). The degree of the approximation is $N_x = N_y = 20$. The left-hand pictures refer to $\sigma = 1$ and the right-hand ones to $\sigma = 1000$.

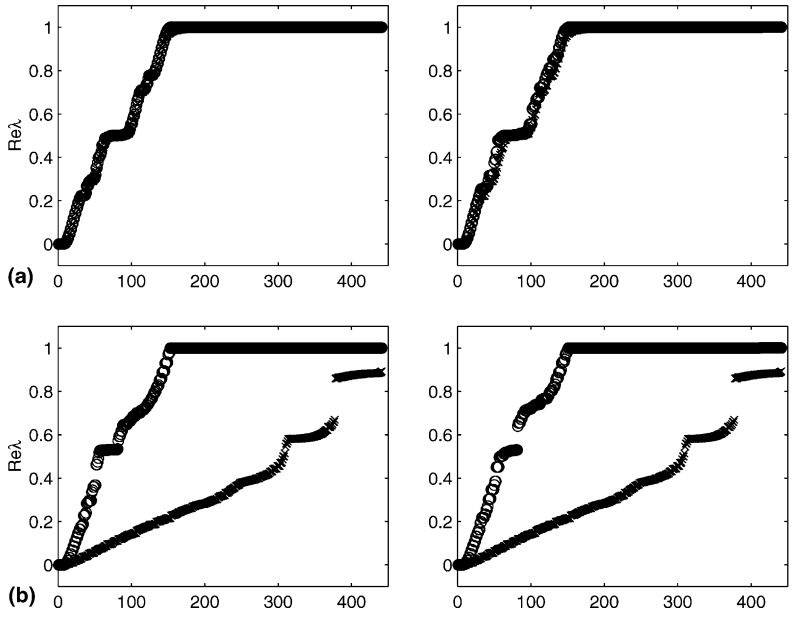

Fig. 2. Distribution of the real parts of the eigenvalues for the three operators in the cases $\sigma = 1$ (a) and $\sigma = 1000$ (b). The degree of the approximation is $N_x = N_y = 20$. The left-hand pictures refer to the pressure operator ($\times$) and the CC operator ($\bigcirc$). The right-hand ones refer to the pressure operator ($\times$) and the FWP operator ($\bigcirc$).

Table 1
Conditioning of the non-preconditioned pressure operator

N	5		10		20	
σ	1	1000	1	1000	1	1000
$\lambda_{\min}$	5.1×10^{-2}	1.87×10^{-3}	1.32×10^{-2}	1.77×10^{-3}	3.22×10^{-3}	1.16×10^{-3}
$\lambda_{\max}$	0.973	3.94×10^{-2}	0.997	0.361	1	0.893
$\kappa(\mathscr{A})$	19.08	21.07	75.55	203.95	310.56	769.83

Table 2
Conditioning of the FWP preconditioned operator

N	5		10		20	
σ	1	1000	1	1000	1	1000
$\lambda_{\min}$	5.29×10^{-2}	4.36×10^{-2}	1.52×10^{-2}	7.75×10^{-3}	3.44×10^{-3}	2.26×10^{-3}
$\kappa(\mathscr{A})$	18.90	22.96	65.79	129.03	290.7	442.48

Table 3
Conditioning of the CC/AIT preconditioned operator

N	5		10		20	
σ	1	1000	1	1000	1	1000
$\lambda_{\min}$	5.19×10^{-2}	2.96×10^{-3}	1.32×10^{-2}	4.57×10^{-3}	3.22×10^{-3}	2.18×10^{-3}
$\kappa(\mathscr{A})$	19.27	337.84	75.76	218.82	310.56	458.72

eigenvalues are still small. As a consequence the global condition number is still bad and it deteriorates as the degree of approximation increases. In Tables 1–3 we report an estimate of the condition number of the operators. The "condition number" κ is defined as the ratio between the maximum absolute value $\lambda_{\max}$ to the minimum absolute value $\lambda_{\min}$ of the eigenvalues. For memory limitation we could not compute the eigenvalues for value of N greater than 20. Observe that for small value of σ the condition number behaves like N^2.

In view of the distribution of the eigenvalues, the bad condition number of the preconditioned operators seems somehow pessimistic. Indeed the few weak eigenvalues that are responsible for the bad condition number are associated to Chebyshev modes of high frequencies. Therefore these eigenvalues may not have any influence on the convergence of the algorithms as long as the residual is higher than the contribution of the last Chebyshev modes in the representation of the divergence. One however expects these eigenvalues to hold back the convergence as the residual becomes sufficiently small. This analysis is confirmed by the numerical results presented in the next section.

6. Numerical experiments

In this section we present results of numerical experiments for both the 2D and 3D GSP. The domain is $\Omega = (-1,1)^d$, $d = 2,3$, and the discretization is done by the Chebyshev collocation method based on the Gauss–Lobatto points (55). For simplicity equal discretization is considered in all directions($N_x = N_y = N_z = N$). The discrete Helmholtz problems for velocity components and the Laplace problem for pressure are solved by the successive diagonalization method [12,13].

We first consider the 2D case.

6.1. The 2D case

The convergence of the iterative procedures is checked against the analytical solution

$$u_1 = \frac{1}{y-2}\mathrm{e}^{(2-x)(y-2)}, \quad u_2 = \frac{1}{x-2}\mathrm{e}^{(2-x)(y-2)}, \quad p = (1-x^2)^2(1+y)(1+\sin(\pi x))\cos(2\pi y), \tag{56}$$

which is divergence free. The forcing term $\mathbf{F}$ in (12) is deduced from the exact solution (56). To start the iterative procedures, we choose an homogeneous pressure. We focus on the decrease of the normalized residual

$$\mathscr{R}^m = \frac{\|\nabla \cdot \mathbf{u}^m\|_\infty}{\|\nabla \cdot \mathbf{u}^0\|_\infty}, \tag{57}$$

where $\|\cdot\|_\infty$ is the discrete infinity norm and $\nabla \cdot \mathbf{u}^0$ is the initial divergence.

In Fig. 3(a), we compare the convergence of the Uzawa and the preconditioned algorithms in the case $\sigma = 1$. Richardson method is used with the same value of ϱ for the three algorithms. (In view of the similarity of the spectrum of the three operators for small σ, it is quite fair to make comparison using the same relaxation parameter.) The degrees of the approximation are $N_x = N_y = 32$. For this small value of σ the Uzawa algorithm and the CC/AIT algorithm have always the same rate of convergence. This is in agreement with the fact that the CC/AIT preconditioner behaves like the identity operator as $\sigma \to 0$ (see the remark at the end of Section 4.1). When ϱ is taken close to value one, the FWP algorithm converges better

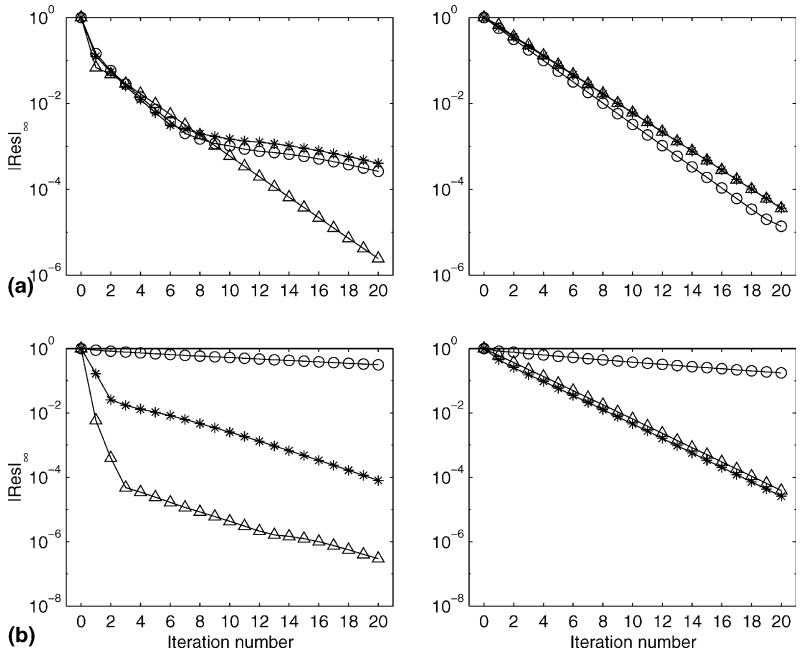

Fig. 3. Convergence history of Uzawa (○), CC/AIT (∗) and FWP (△) algorithms for the 2D GSP with the degrees of approximation $N_x = N_y = 32$. Richardson method is used with $\varrho = 1$ (left-hand pictures) and $\varrho = 1.6$ (right-hand pictures). Pictures (a) refer to the case $\sigma = 1$ and pictures (b) to the case $\sigma = 1000$.

than the Uzawa and the CC/AIT algorithm, though initially the three algorithms have a similar rate of convergence. The convergence of the Uzawa and the CC/AIT algorithms improves if we take values of ϱ bigger than one and with $\varrho = 1.6$ both preconditioned methods give virtually the same results. Note that as ϱ increases the rate of convergence of FWP method decreases. Actually in the first iterations the reduction factor of the three algorithms behaves like $\|\nabla \cdot \mathbf{u}^{m+1}\|_\infty / \|\nabla \cdot \mathbf{u}^m\|_\infty \simeq \varrho - 1$. This means that in the first iterations, the algorithms behave as if the condition number of the operators were one.

The results in Fig. 3(b) obtained with $\sigma = 1000$ and $N_x = N_y = 32$ show that for large σ, the convergence of the Uzawa algorithm becomes very slow. Now both preconditioned methods improve substantially the convergence. Also as for the case $\sigma = 1$, the FWP algorithm converges better than the CC/AIT if the relaxation parameter is taken close to value one. Note however that the convergence of the FWP method slows down as the residual becomes small confirming the analysis at the end of Section 5.

In Fig. 4, we show the influence of the discretization on the convergence of the algorithms. The Richardson method is used with $\varrho = 1$. One can see that the convergence of the FWP method improves as the degree of the approximation increases. In contrast the convergence of the CC/AIT method deteriorates as the discretization becomes finer.

Now we consider the dynamical methods. We first compare PMR method with QPMR method when they are associated to each preconditioned algorithm. For the CC/AIT method, we found that both choices of relaxation parameter always lead to similar results (see Fig. 5(a)). The two methods also lead to similar results if σ is sufficiently large in the case of the FWP algorithm. However, for small value of σ we found that the QPMR method gives better results (see the case $\sigma = 1$ in Fig. 5(b)). The same behavior is observed when we change the degree of approximation.

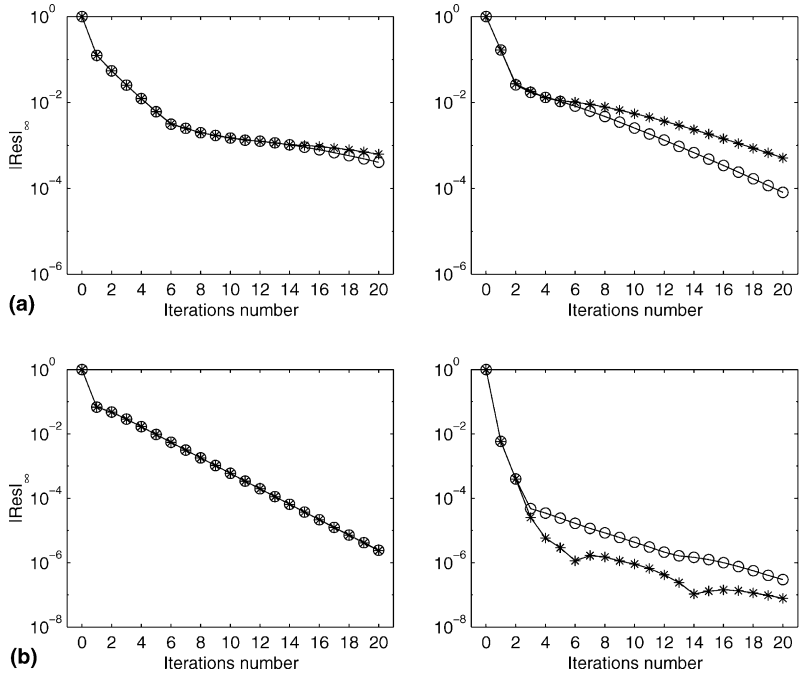

Fig. 4. Convergence history of CC/AIT algorithm (a) and FWP algorithm (b) for the 2D GSP with the degrees of approximation $N_x = N_y = 32$ (○) and $N_x = N_y = 64$ (∗). Richardson method is used with $\varrho = 1$. The left-hand pictures correspond to the case $\sigma = 1$ and the right-hand one to the case $\sigma = 1000$.

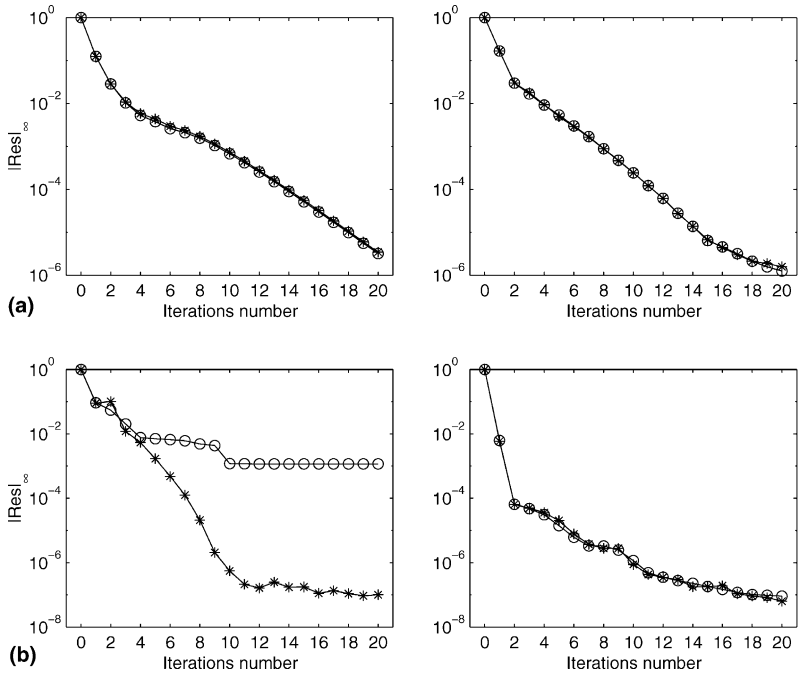

Fig. 5. Convergence history of CC/AIT algorithm (a) and FWP (b) algorithm for the 2D GSP with the degrees of approximation $N_x = N_y = 32$. The PMR (○) and the QPMR (∗) methods are used. The left-hand pictures correspond to the case $\sigma = 1$ and the right-hand ones to $\sigma = 1000$.

In Fig. 6, we compare the convergence of the algorithms when the QPMR method (quasi-minimal residual "QMR" in the case of the Uzawa algorithm) is used. Here too, the results obtained by Uzawa and CC/AIT algorithms are very close when σ is small. The behavior of the algorithms is quite similar to the case $\varrho = 1$ in the static Richardson method. The superiority of FWP over the CC/AIT method becomes clear particularly when σ becomes large. Note again the slowing down of the FWP algorithm as the residual becomes small.

Next we present some numerical experiments for the 3D GSP.

6.2. The 3D case

The convergence of the algorithms is checked against the exact solution

$$u_1 = \frac{(5+x)^5}{y-2} e^{(2-x)(y-2)(1+z)}, \quad u_2 = \frac{(3+y)^5}{x-2} \cos(\pi z) e^{(2-x)(y-2)},$$
$$u_3 = \frac{(5+z)^5}{2-x} \cos(2\pi z) e^{(2-x)(y-2)}, \quad p = 2(1-x^2)^2(1+y)(1+\sin\pi x)\cos(2\pi y)(1+z^3)e^{1+z}. \tag{58}$$

As before the exact solution gives the forcing terms in the Generalized Stokes problem (12) and (13). Moreover this solution (58) is not divergence free and therefore a non-homogeneous term is also added for the continuity equation. To start the iterative procedures we select as previously a homogeneous pressure field.

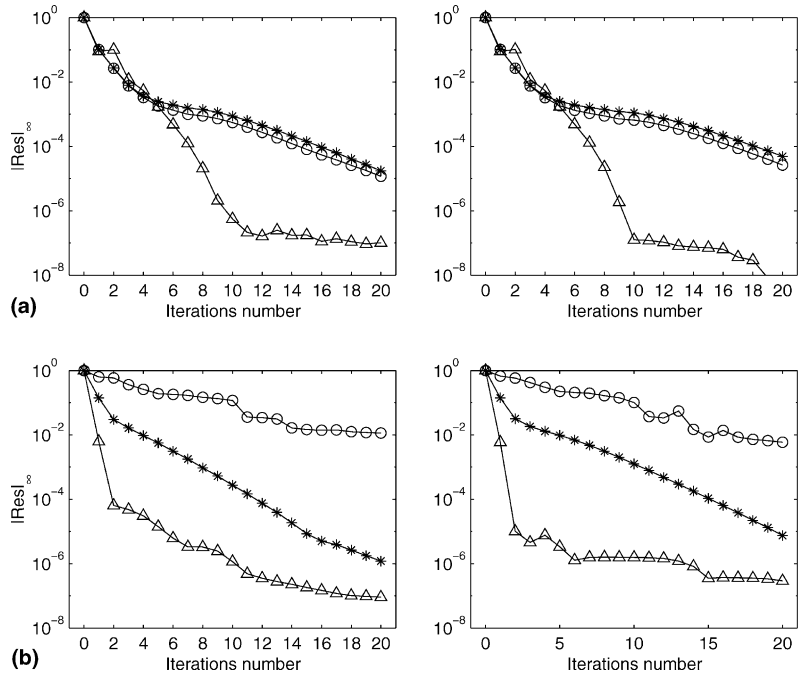

Fig. 6. Convergence history of Uzawa (○), CC (∗) and FWP (△) algorithms for the 2D GSP in the cases $\sigma = 1$ (a) and $\sigma = 1000$ (b). The QPMR method is used. The left-hand pictures correspond to the approximation $N_x = N_y = 32$ and the right-hand side ones to $N_x = N_y = 64$.

As the results for the 3D case are quite similar to those for the 2D case, we only present results obtained with the PMR. Here for both FWP and CC/AIT algorithms, the PMR and QPMR methods always give similar results.

In Fig. 7 we compare the convergence of the various algorithms when associated to the PMR method (MR in the case of the Uzawa algorithm). Here too, the FWP method has the best rate of convergence. As for the 2D case, the convergence of the FWP method slows down when the residual reaches a certain level of precision. Here the level is is slightly higher because the exact solution (58) is more complex than the exact solution (56) in the 2D case.

Thus for both the 2D and 3D cases, the preconditioned methods give satisfactory results. The best results being obtained when the FWP method is employed. This shows that the modification of the boundary conditions for the velocity in the case of FWP method plays a beneficial role for the convergence. The eigenvalues analysis in conjunction with the convergence history indicate that the slowing down of the FWP algorithm at low residual reflects the effect of weekly spurious eigenvalues. As these eigenvalues are associated to Chebyshev modes of high order, they can influence the convergence only at low residual. This argument is supported by the fact that, when the degree of approximation increases, the residual decreases to a lower level before the algorithm stagnates. This suggests an improvement of the FWP algorithm by using a filtering procedure to remove the highest Chebyshev modes from the pressure. This will be the subject of the next section. The same argument however does not hold for the CC/AIT method. Indeed in some cases (Fig. 3 for instance), we do observe a change in regime of convergence of the CC/AIT algorithm, but it occurs when the residual is too high for this to reflect the convergence of the last Chebyshev modes. Moreover, we saw that the convergence of the CC/AIT algorithm deteriorates as the degree of approximation increases.

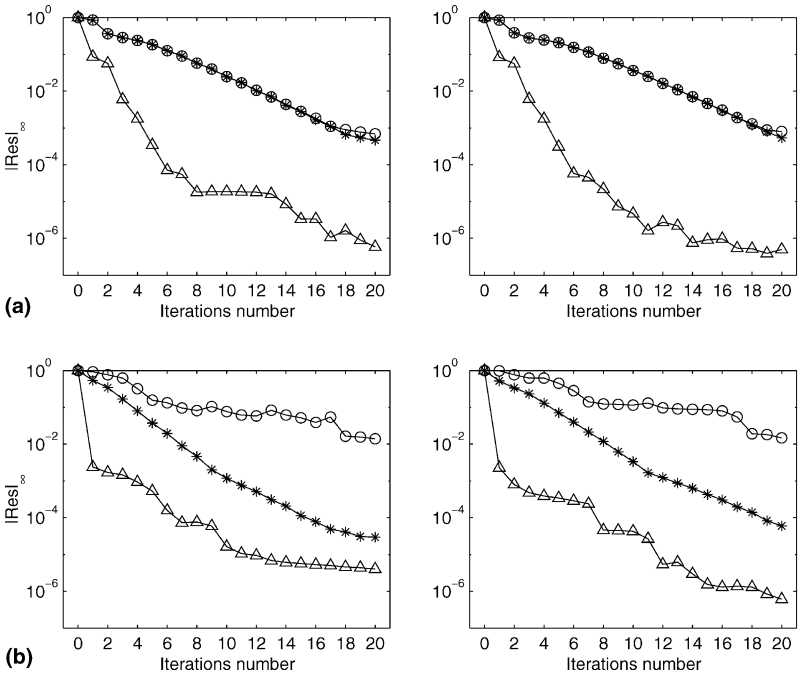

Fig. 7. Convergence history of Uzawa (○), CC/AIT (∗) and FWP (△) algorithms for the 3D GSP with the degrees of approximation $N_x = N_y = N_z = 24$ (left-hand pictures) and $N_x = N_y = N_z = 32$ (right-hand pictures). Pictures (a) refer to the case $\sigma = 1$ and pictures (b) to the case $\sigma = 1000$. PMR method is used.

6.3. Enhancement of the FWP preconditioning

The use of half-staggered grid can partly overcome the problem of the spurious and weakly spurious modes (i.e., the modes with small eigenvalues). The pressure is represented by polynomials of degree $N-1$ in both directions and the continuity equation is imposed on the $N \times N$ Gauss points $[\cos((2i+1)\pi/2N), \cos((2j+1)\pi/2N)]$, $1 \leqslant i, j \leqslant N$. This procedure is known to contain only a single spurious mode. In addition this discretization still contains some weakly spurious modes. Since the slowing down of the convergence is related to the weakly spurious modes (we recall that the strictly spurious modes have no influence on the convergence since these modes are filtered by the divergence operator) this discretization may not lead to a significant improvement of convergence. Therefore a procedure which allows also a filtering of the weak eigenvalues is much suitable. This can be achieved by using a representation of pressure on Gauss–Lobatto points $[\cos(i\pi/(N-K)), \cos(j\pi/(N-K))]$, $0 \leqslant i, j \leqslant N-K$, where K is an integer greater than 1 and less than N. Chebyshev interpolation is used to move from a grid to another. Let $\mathscr{R}$ be the interpolating operator which transfers variables from the finest grid to the coarse grid and $\mathscr{P}$ the operator that performs the reverse process. Then the proposed procedure is the following:

Starting from a pressure field p^m:

1. Filtering $\tilde{p} = \mathscr{P}\mathscr{R}p^m$.
2. Solve $\mathscr{H}_b \mathbf{u}^{m+1} = \nabla\tilde{p}$.
3. Compute $\Delta_b \delta p^{m+1} = \mathscr{H}(\nabla \cdot \mathbf{u}^m)$.
4. $p^{m+1} = p^m + \varrho_m \delta p^{m+1}$.

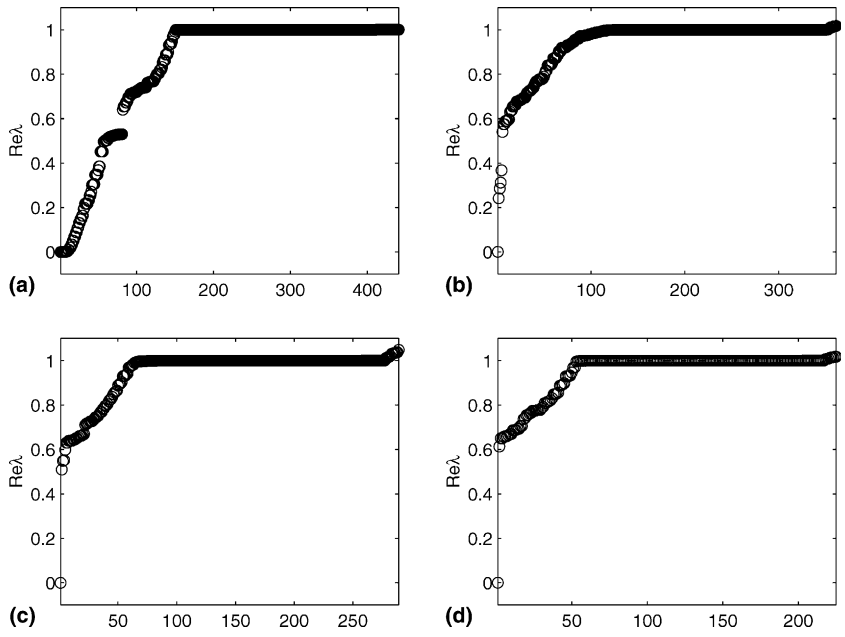

Fig. 8. Distribution of real parts of the eigenvalues for the FWP operator in the case of the approximation P_N (a), P_{N-2} (b), P_{N-4} (c) and P_{N-6} (d), $N = 20$ for the pressure.

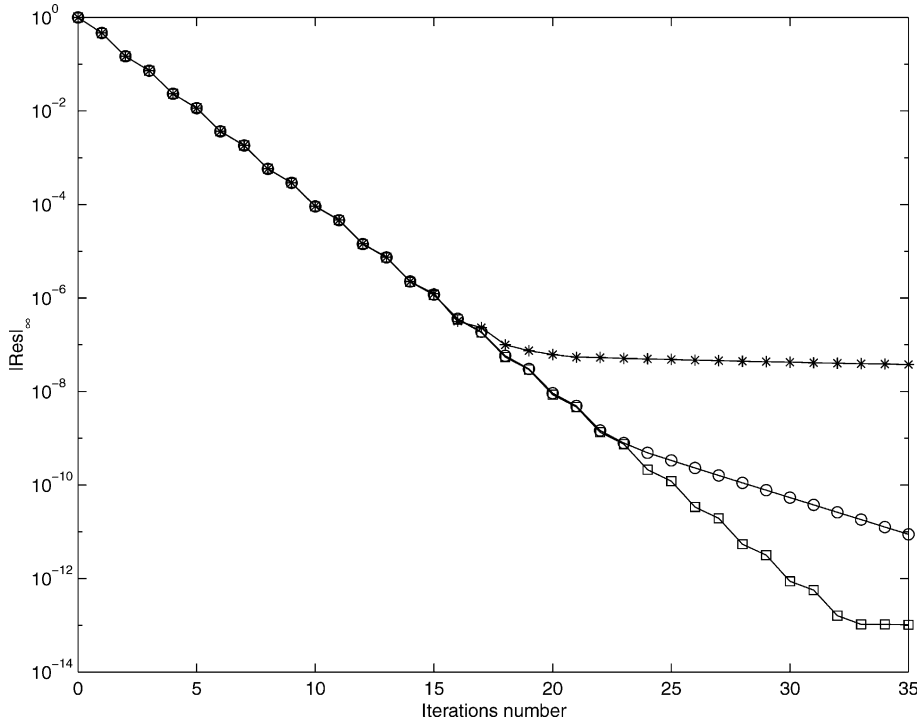

Fig. 9. Convergence history of FWP algorithm for the 2D GSP with $\sigma = 1$ and approximations P_N (∗), P_{N-2} (○) and P_{N-4} (□), $N = 32$ for the pressure. Richardson method is used with $\varrho = 1.4$. The data are defined by the smooth solution (56).

In step 1, applying operator $\mathscr{P}\mathscr{R}$ has the effect of removing the last K Chebyshev modes of the pressure. Thus at each iteration a filtering procedure is applied to remove the last Chebyshev modes of pressure before the computation of velocity. Observe that in step 2 the pressure is actually computed on the finest grid. Indeed, in the FWP method, values of the normal velocity are used as boundary conditions for pressure. Therefore if the pressure were computed on the coarse grid, after convergence of the algorithm, the Dirichlet boundary condition on the normal velocity component would be satisfied only on the coarser grid and this is not convenient.

When the filtering procedure is applied with $K \geqslant 2$, all the non-constant spurious modes are eliminated. Moreover (and this is important in view of what has been previously said) as K increases, the smallest non-zero eigenvalues are eliminated, thus resulting to better conditioning. This can be seen in Fig. 8 where the real parts of the eigenvalues are reported. Few of the eigenvalues are still complex with relatively small imaginary part. The results in Fig. 8 correspond to $\sigma = 1000$ and $N = 20$. Similar results are obtained with small σ.

The validity of the present approach has been checked by conducting numerical experiments in 2D with both smooth and non-smooth data.

The smooth data are obtained from the analytical velocity and pressure (56) as in Section 6.1. In Figs. 9 and 10 we report results corresponding to the case $\sigma = 1$ and $\sigma = 1000$, respectively. In both cases we used the static Richardson method with $\varrho = 1.4$ and the degrees of approximation $N_x = N_y = 32$. It can be seen that the different filterings virtually lead to the same rate of convergence during the first iterations. After this stage the convergence slows down when the high modes are retained for the pressure. The convergence

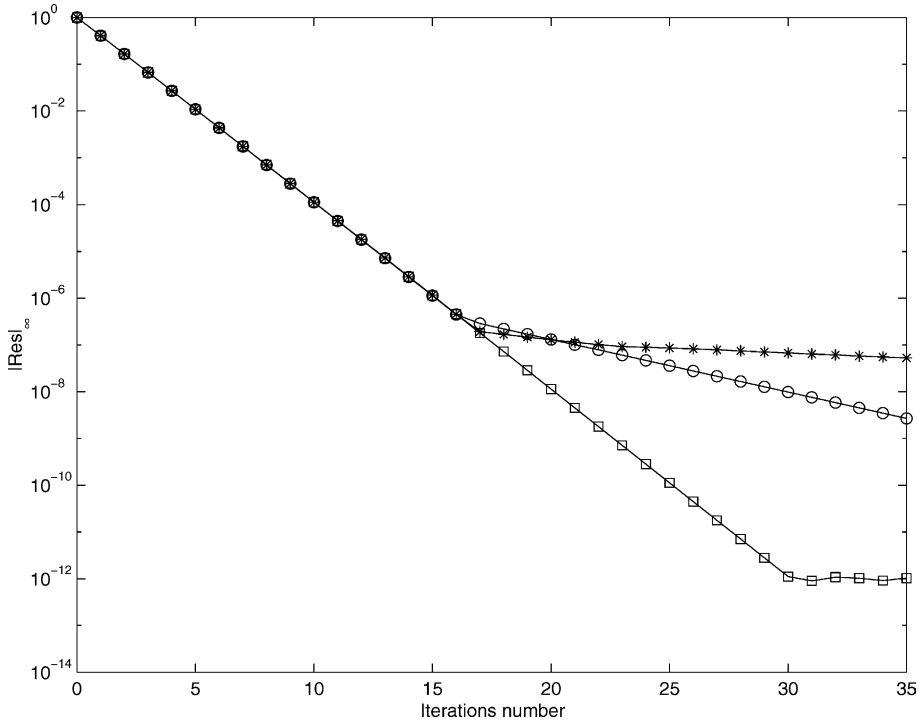

Fig. 10. Convergence history of FWP algorithm for the 2D GSP with $\sigma = 1000$ and approximations P_N (∗), P_{N-2} (○) and P_{N-4} (□), $N = 32$ for the pressure. Richardson method is used with $\varrho = 1.4$. The data are defined by the smooth solution (56).

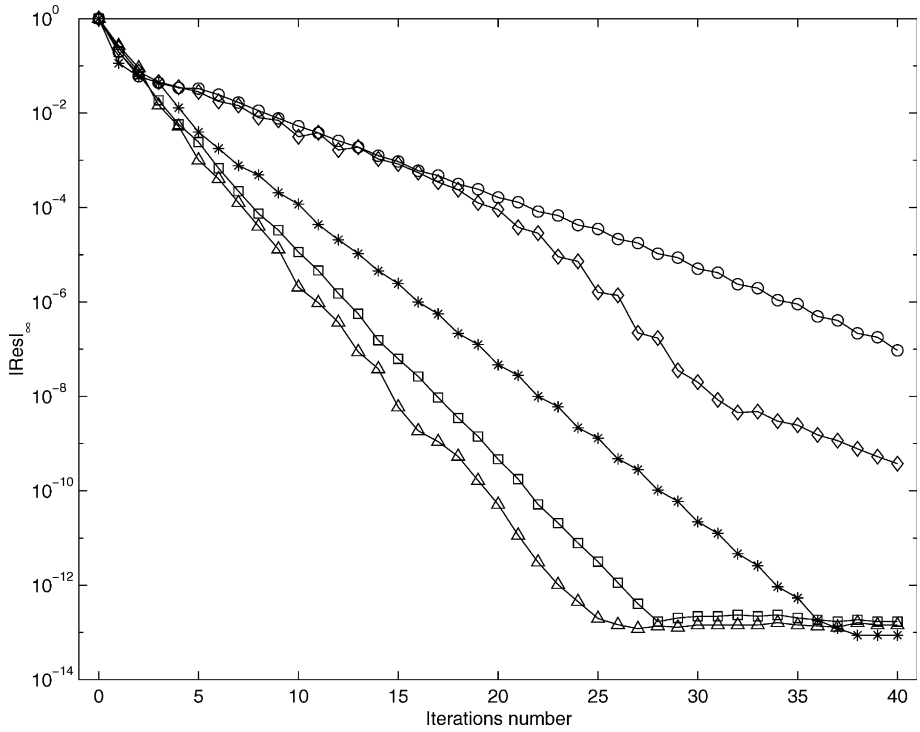

Fig. 11. Convergence history of FWP algorithm for the 2D GSP with $\sigma = 1000$ and approximations P_N (○), P_{N-2} (◇) and P_{N-4} (∗), P_{N-6} (□) and P_{N-8} (△), $N = 32$ for the pressure. The PMR method is used. Non smooth exact pressure data are used (see Section 6.3).

is then gradually improved when we use filterings with increasing value of K. Of course beyond a certain value of K, no further improvement is obtained.

In Fig. 11, we show results of the filtering when non-smooth data are used. The non-smooth data are obtained by choosing randomly the Chebyshev coefficients of the exact pressure in interval $]0, 1[$. The exact velocity is still given by (56). Here we have used the PMR method. We observe the same improvement of the rate of convergence as K increases. Note that here the bifurcation among these different curves of convergence occurs earlier because the coefficients of the last Chebyshev modes of the pressure can be relatively high.

It should be noticed that in practice the procedure for filtering the parasitic modes does not work well in the case of the CC/AIT preconditioning confirming our argument at the end of Section 6.2.

7. Conclusion

Two iterative approaches for solving the GSP has been analyzed and implemented in the framework of collocation Chebyshev approximation. The iterative procedures use two kinds of preconditioning for the Uzawa algorithm. One of them, the AIT/CC method is a reformulation of the preconditioning due to Cahouet and Chabard [6] in the case of finite elements discretization. This method has the advantage of being applicable in arbitrary domain and it leads to accurate results when associated to conjugated gradient method. However even with the lack of symmetry of the collocation Chebyshev version of the operator, we obtained quite satisfactory results when the AIT/CC is associated with the static Richardson or PMR like

methods. The second preconditioning considered, the FWP method is restricted to rectangular domains. For such geometries we found this method well suited when associated to spectral Chebyshev methods. Comparison of the two preconditioning shows an advantage of the FWP method over the AIT/CC method. However, we noted that the convergence of the various preconditioned algorithms slows down as the residual becomes small. This is due to the fact that, though the direct application of the preconditioning results in a clustering of the eigenvalues about unity, it does not eliminate the weekly spurious eigenvalues that are related to the last Chebyshev modes. Thanks to an suitable filtering process, it has been possible to remedy to this situation for the FWP algorithm only (the filtering enhancement does not work for CC/AIT preconditioning). The filtering consists in removing the last modes of the Chebyshev expansion of pressure field. Numerical tests with both smooth and non-smooth (i.e., random) data confirm the effectiveness of the filtering procedure.

References

[1] L. Kleiser, U. Schumann, Treatment of the incompressibility and boundary conditions in 3-D numerical spectral simulations of plane channel flows, in: E.H. Hirschel (Ed.), Proc. 3rd GAMM Conf. Numerical Methods in Fluid Mechanics, Vieweg, Braunschweig, 1980, pp. 165–173.
[2] P. Le Quéré, Aziary de Rocquefort, Sur une méthode semi-implicite pour la résolution des équations de Navier–Stokes d'un écoulement visqueux incompressible, C.R. Acad. Sci. Paris, série II 294 (1982) 941–944.
[3] L. Tukerman, Divergence-free velocity in nonperiodic geometries, J. Comput. Phys. 80 (1989) 403–441.
[4] P. Haldenwang, Unsteady numerical simulation by Chebycshev spectral methods of natural convection at high Rayleigh number, in: J.A.C. Humphrey (Ed.), Significant questions in buoyancy affected enclosure or cavity flow, ASME/HTD, 60, 1986, pp. 45–51.
[5] P. Haldenwang, G. Labrosse, 2-D and 3-D spectral Chebyshev solutions for free convection at high Rayleigh number, in: M.O. Bristeau, R. Glowinski, A. Haussel, J. Periaux (Eds.), Proc. 6th Int. Symp. on Finite Elements in Flow Problems, Antibes, France, 1986, pp. 261–266.
[6] J. Cahouet, J.P. Chabard, Some fast 3D finite elements solver for the generalized Stokes problem, Int. J. Numer. Meth. Fluids 8 (1988) 869–895.
[7] A. Majda, J. Sethian, The derivation and numerical solution of the equations for zero Mach number combustion, Combust. Sci. Technol. 42 (1985) 185–205.
[8] J. Fröhlich, R. Peyret, Direct spectral method for the low-Mach number equations, Int. J. Numer. Methods Heat and Fluid Flow 2 (1992) 195–213.
[9] B. Denet, P. Haldenwang, Combust. Sci. Technol. 104 (1995) 143–167.
[10] R. Glowinski, Ensuring well-posedness by analogy; Stokes problem and boundary control for the wave equation, J. Comput. Phys. 103 (1992) 189–221.
[11] A. Garba, *Méthodes Spectrales en Domaines non Rectangulaires: Applications au Calcul d'écoulements á Surface libre*, Thèse de l'Université de Nice–Sohia Antipolis, France, 1993.
[12] P. Haldenwang, G. Labrosse, S. Abboudi, Chebyshev 3-D Spectral and 2-D pseudospectral solvers for the Helmholtz equation, J. Comput. Phys. 55 (1984) 115–128.
[13] U. Ehreinstein, R. Peyret, A Chebyshev-collocation method for Navier–Stokes equations with application to double-duffision convection, Int. J. Numer. Methods Fluids 9 (1989) 429–452.
[14] C. Canuto, M.Y. Hussaini, A. Quateroni, T.A. Zang, Spectral Methods in Fluid Dynamics, Springer, New York, 1988.